Multi-Phase Cage Rotor Induction Machine Drive with Direct Implementation of Brush DC Operation

Nkosinathi Gule and Maarten J. Kamper, SMIEEE
Dept. of Electrical and Electronic Engineering
University of Stellenbosch
Stellenbosch, South Africa
E-mail: nathie@sun.ac.za, kamper@sun.ac.za

Abstract—**In this paper, a multi-phase induction machine drive utilising the brush dc machine operation principle is presented and implemented on a cage rotor multi-phase induction machine. The results from measurements prove that the proposed brush dc control method for multi-phase induction machine drives produces remarkable results in the sub-base and flux weakening speed regions of the drive. It is found that a lower number of number of field phases can be used for better use of the inverter current capability and for better current density distribution. Also, results show that the drive system's efficiency compares well with that of a standard three phase drive system. The method can be used for any high-phase-number cage or wound rotor induction machines.**

I. INTRODUCTION

Multi-phase induction machine drives possess several advantages over conventional three phase induction machine drives in high-power applications [1-10]. Besides better fault tolerance and higher reliability, the advantages of multi-phase induction machines include

(i) reduction in the
- amplitude of torque pulsation,
- rotor harmonic currents,
- current per phase without increasing the phase voltage,
- dc link current harmonics, and

(ii) and an increase in the
- machine power and torque per rms current for the same volume machine, and,
- torque pulsation frequency.

Depending on the stator winding, other advantages are: independent control of multimotor multiphase drive systems with a single power electronic converter supply and torque enhancement through stator current harmonic injection. Also, a higher phase number leads to the improvement of the quality of the air-gap flux density waveform regardless of the current waveform or winding design, because with a higher phase number there is less interaction between space and time harmonics.

At present, multiphase induction machines are used in highly specialized applications such as locomotive traction, electric and hybrid-electric vehicles, industrial high power applications, electric ship propulsion [5], [11] and the more electric aircraft [12-14]. Battery powered applications such as cordless power tools and small traction drives are also considered [15].

Speed control methods of multi-phase induction machine drives are similar to those of three phase induction machine drives. Scalar control has lost popularity, whilst more interest is now shown in vector and direct torque control (DTC) due to the higher cost of multi-phase power electronics when compared to the cost of implementing control algorithms [4]. However, the currently employed control techniques are quite complex as coordinate transformations and model representation of the multi-phase induction machine become more demanding [1],[4].

Recently, a control method that does not require any coordinate transformation for a six-phase induction machine drive was proposed and evaluated [16]. This control method is in effect a direct implementation of the operation of a brush dc machine with compensating windings, i.e. by using the stator phase windings to act alternately as flux or torque producing phases. The control method is proved to work remarkably well from practical measurements on a two-pole, six-phase, wound rotor induction machine drive.

In this paper, the machine drive and control method of [16] is further investigated and evaluated on a 11 kW, nine-phase, cage rotor induction machine drive. In particular the effect on the ratio of the number of field (flux) to torque phases is investigated and confirmed by measurements. The application of this type of drive is only for very-high-power variable speed drive applications, e.g. in the 50 MW power level. In this paper, the control method is termed the "brush dc equivalent" (BDCE) control method.

II. BRUSH DC EQUIVALENT (BDCE) METHOD

The operation principle of BDCE control and a method of finding the static torque of a BDCE controlled induction machine are presented in this section.

A. Operation Principle

The principle of operation of the BDCE multiphase induction machine drive is best explained graphically. The configuration of the stator phase current waveforms shown in Fig. 1 allows separate rotating flux or field MMF with an amplitude, F_f, and torque MMF with an amplitude, F_t, in a two pole six-

phase induction machine. In the figure, it is shown that the stator phase current consists of trapezoidal-shaped field and torque current components, with flat-topped amplitudes of I_f and I_t respectively. That is, a stator phase acts alternately in time as either a flux or a torque producing phase. Furthermore, it can be seen from Figs. 1 and 2 that at any instant there are always three neighbouring stator phase windings that act as field windings to generate the flux in the machine whilst the other three neighbouring stator phase windings always act as torque windings to generate the torque of the machine. The generated flux in the machine will lead to induced rotor phase voltages and currents at slip speed. The rotor currents produce the rotor MMF, F_r. The torque current flowing in the torque producing stator phases, however, produces a counter MMF that balances the rotor MMF during operation of the BDCE controlled multiphase induction machine. Fig. 3 is obtained from Fig. 2, with $F_t = F_r$ and $\alpha = 0$ for balanced MMF condition (flux decoupling condition). There is, thus, an important relationship between the torque current, I_t, and the angular slip frequency, ω_{sl}, for balanced MMF control (or decouple control), that is

$$k = \frac{\omega_{sl}}{I_t}. \tag{1}$$

The relationship given by (1) is used in the control system, where k is used as a control gain. The control gain, k, also depends on the physical dimensions of the machine, the total number of phases, the rotor phase resistance and the air-gap flux density [16].

Fig. 4 shows a block diagram of a six-phase induction machine drive with its control system. Similarly to [17] and to phase redundant multiphase systems [2], a full bridge inverter is used for each stator phase winding, which results in twelve phase legs for the six-phase drive. The rotor speed together with the phase currents of the drive are measured and fed back to a digital signal processor (DSP) controller. The field current is kept constant under base speed. The speed controller controls the torque command-current I_t from which the slip angular frequency ω_{sl} is determined using the control gain, k, of (1). From this and from the known field command current I_f, the six reference phase currents of the drive are generated. A digitally implemented hysteresis current regulator, using a field programmable gate array (FPGA), is used for the current control. The switching signals are sent to the inverter via fibre optic cables. The advantage of this method is that it does not require any transformations and model representations such as in vector control and DTC.

B. *Analysis*

From Figs. 1 to 3, it is clear that, at any time instance, the amplitude of the field MMF, F_f, is

$$F_f = 2N_s I_f, \tag{2}$$

where N_s is the number of turns in series per phase. Similarly, the amplitude of the torque MMF is

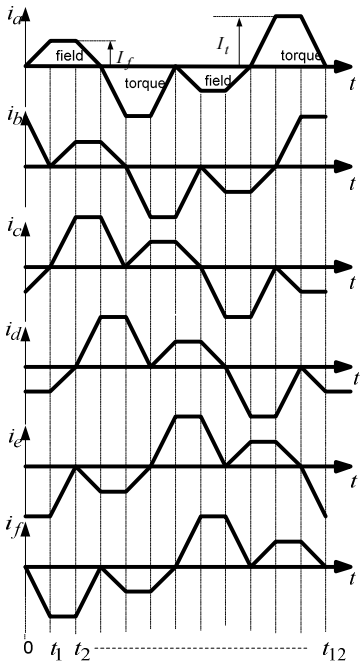

Fig. 1. Trapezoidal six-phase current waveforms [16].

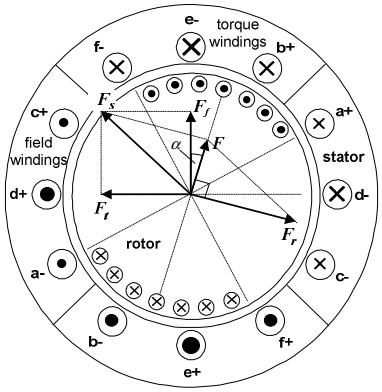

Fig. 2. Current distribution and MMF space phasors at time t = t1/2 [16].

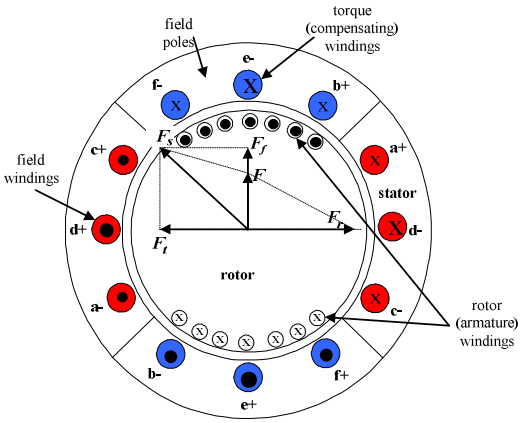

Fig. 3. Current distribution and MMF space phasors when α = 0.

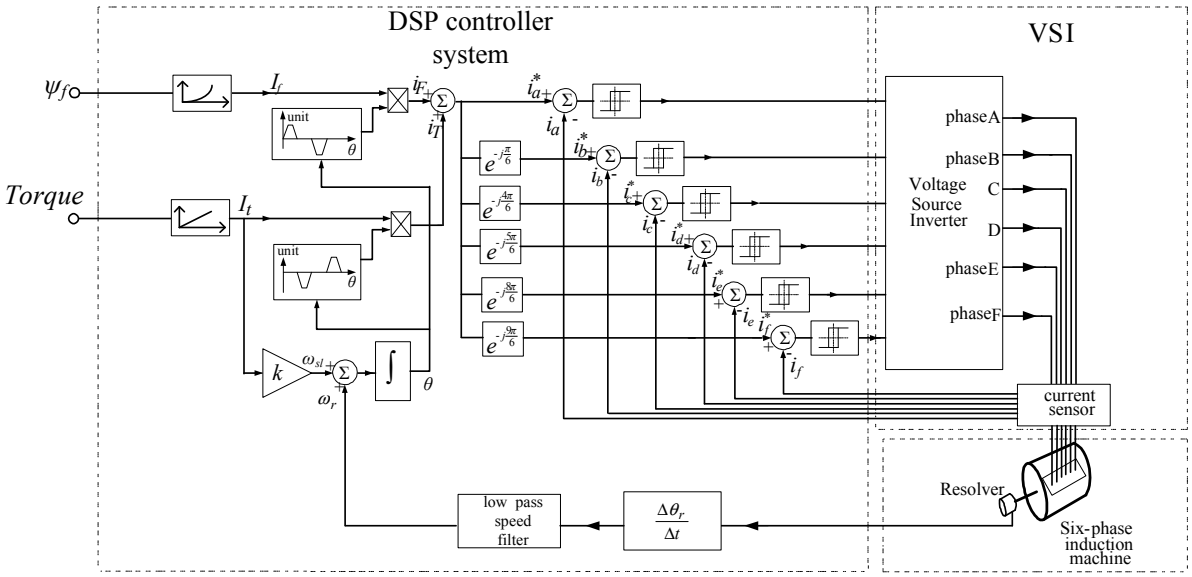

Fig. 4. BDCE control system operation of a six-phase induction motor [16].

$$F_t = 2N_s I_t \,. \tag{3}$$

In the analysis, assuming perfect commutation and quasi-square-wave air-gap flux density, the induced rotor phase current waveform will have an ideal square-like form as shown in Fig. 5. With the position of the active rotor phase windings opposite the position of the compensating or torque phase winding of the stator, the rotor MMF amplitude is given by

$$F_r = m_{ra} N_r I_r \,, \tag{4}$$

where, m_{ra} is the number of active bars or rotor phases underneath a pole at any time instance and N_r is the number of turns in series per rotor phase, (N_r = 0.5 for cage rotor). Theoretically, the number of active bars per pole is

$$m_{ra} = \frac{M_r (m_t - 1)}{2N_p p} \,, \tag{5}$$

where M_r is the number of rotor bars, m_t is the number of torque phases, $N_p = m_t + m_f$ and p is the number of pole pairs.

The rotor phase winding or bar induced voltage waveform assumes a near square due to the quasi-square air-gap flux density. The flat-topped amplitude of this waveform can be calculated similarly to that of dc machines as

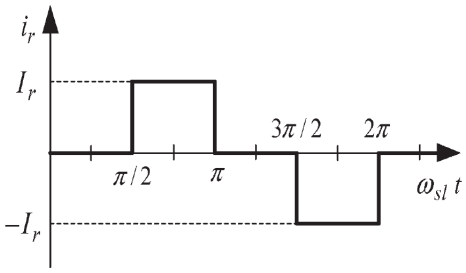

Fig. 5. Assumed rotor current with number of field phases equal to the number of torque phases in a six-phase induction machine [16].

$$E_b = 2N_r B l \omega_{sl} r_g \,, \tag{6}$$

where ω_{sl} is the angular slip frequency, B is the air-gap flux density, l is the stack length, and r_g is the air-gap radius. The induced rotor bar current is given by

$$I_r = \frac{E_b}{R_b} = \frac{2N_r B l \omega_{sl} r_g}{R_b} \,, \tag{7}$$

where R_b is the rotor phase resistance. Using Lorentz force law, similarly to the brush dc machine case, the electromagnetic torque of the machine is given by

$$T = 2m_{ra} N_r r_g l B I_r \,. \tag{8}$$

Under balanced MMF conditions ($F_t = F_r$), using (3), (4) and (8) it can be shown that

$$T = 4N_s r_g l B I_t \,. \tag{9}$$

Thus, there is a linear relationship between torque and the torque current, I_t, similar to the linear relationship between torque and armature current in dc machine theory.

Considering MMF balance, the control gain can be evaluated as

$$k = \frac{\omega_{sl}}{I_t} = \frac{(m_t - 1) N_s R_r}{4 p m_{ra} N_r^2 B l r_g} \,. \tag{10}$$

III. Nine-phase Cage-Rotor Induction Machine Drive Evaluation

A nine-phase cage rotor induction machine drive is developed using the proposed control method of Section II. A cage rotor is specifically selected in this case, as [16] uses a wound rotor – it is important to know if additional copper loss is generated in the cage rotor due to the trapezoidal stator currents.

A standard 11 kW, four-pole, 36-slot, three-phase induction machine stator is rewinded to a nine-phase stator with full-pitch coils. The rewinded stator is shown in Fig. 6. The original

28-slot aluminium cage rotor of the three-phase induction machine is used for the rotor of the nine-phase induction machine. Additional parameters of the nine-phase machine are given in Table 1.

The inverter comprises of Intelligent Power Modules (IPMs), the control and isolated power circuits, the bus bar and per phase current sensors. Modular design is utilised in the design of the inverter since it allows for independent testing and simple replacement of faulty boards. An H-bridge is required for each phase of the nine-phase machine, thus, the inverter consists of six 6MBP25RA120 three-phase intelligent power modules (IPMs). Each control board is shared by two IPMs. The hardware and software of the DSP system of Fig. 4 is expanded to become a nine-phase control system. The nine-phase trapezoidal stator current waveforms are generated similarly to the six-phase waveforms described in section II. Based on the method presented in [18], the optimal (best) ratio of the number of field phases to torque phases,

$$m = m_f/m_t, \tag{11}$$

is calculated to be $m = 0.5$ (that is, $m_f = 3$ and $m_t = 6$), which is in contrast with $m = 1$ ($m_f = 3$ and $m_t = 3$) that is used in [16].

Fig. 7 shows a schematic of the experimental setup built to test the nine-phase induction machine. A three-phase 37 kW induction machine is used as a load drive. During testing, the induction machine load drive is kept at a constant speed through the Powerflex 700 drive. The nine-phase DSP control system measures the rotor speed and produces the PWM signals that drive the inverter. The torque is measured through a torque transducer installed on the shaft linking the two machines.

IV. Measurement Results

In Fig. 8 the measured current waveforms of the nine-phase induction machine drive at rated speed and rated flux, and at double rated speed and flux weakening are shown. With a flat-topped back-EMF phase voltage of 400 V at rated frequency and rated flux, and with V_{dc} = 400 V, the drive shows good flux weakening operation (Fig. 8 – red curve), just as in a brush dc machine. The current waveforms show that the current controller works well even at double rated frequency.

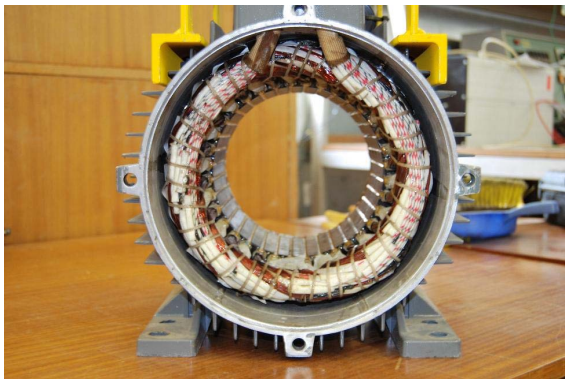

Fig. 6. Stator of the nine-phase induction machine.

Table 1. Machine Parameters of a 4-pole 9-phase Induction Machine.

Rated Power, P_n	11kW
Air-gap length, g	0.5 mm
Stack length, l	127 mm (copper bars)
Rotor radius, r_g	84.5 mm
End ring segment resistance, R_e	1.28e-6 Ω (75°C)
End ring segment inductance, L_{er}	29.2 nH
Number of field phases, m_f	3
Number of torque phases, m_t	6
Number of rotor bars, M_r	28
Number of stator slots, M_s	36
Number of series turns per stator phase, N_s	170
Air-gap flux density, B	0.7 T
Rated I_f	5.83 A
Rated I_t	5.5 A
Rated k	0.638 rad/As
Rated speed	1466 r/min

The slip is clearly seen in the results. The results further confirm the brush dc compensating winding operation of the control method. Note that k of (1) is adjusted in the field weakening speed range since it depends on the flux density. Fig. 9 shows the advantage of taking $m = 3/6 = 0.5$ over $m = 4/5 = 0.8$, as the inverter phase current during field and torque operation is more even, and so also the peak slot current density. In Fig. 10, the comparison of the measured and analytically calculated torque results of the drive are shown at rated field current, I_f = 5.83 A, and with a rated control gain value, k = 0.638. In this measurement, the rotor speed is 500 r/min and the expression for evaluating the analytically calculated torque of the BDCE controlled nine-phase four pole machine is given by

$$T = 2(m_t - 1)N_s I_t B l r_g . \tag{12}$$

This expression is developed in a similar fashion to that in equation (9). Both results show a linear relationship between the torque current and the developed torque. The figure shows that at the rated torque current value (I_t = 5.5 A), the measured and calculated torque values are more or less the same. Nonetheless, the result shows that the drive maintains balanced MMF condition regardless of the torque current. This proves the BDCE operation of the machine.

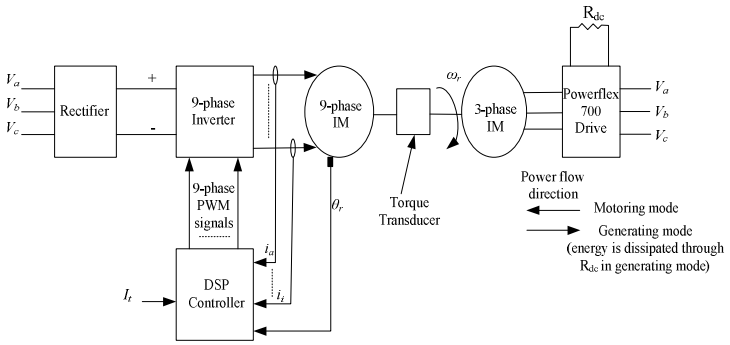

Fig. 7. Test bench setup schematic.

The linear relationship between the measured torque and torque current is achievable at rated speed as shown in Fig. 11. In this figure there is a slight difference between the analytically calculated torque and the measured torque. This may be a result of increased friction and windage losses, and other stray-load losses; the analytically calculated torque is the developed torque whilst the measured torque is the shaft torque of the machine.

The measured results of Fig. 12 show a low torque sensitivity to the k value, which is good, since k is a function of rotor resistance which changes with temperature. Also, at higher than rated torque current, a small change in k from the rated k-value leads to a reduction in torque as shown for I_t = 7.5 A. Fig. 13 shows that there is a slight advantage in terms of efficiency of the system (converter and induction machine) in using m = 0.5 than with m = 0.8. Also in the figure, the 84 % overall drive efficiency obtained at full load can be considered as very good, compared to 85 % of the standard three-phase drive also shown. In Fig. 14, the measured torque is shown at different frequencies with the appropriate field current in the flux weakening speed (frequency) region. The measured torque at a rotor speed of 3000 r/min is 36 Nm, whilst it is 67 Nm at 1500 r/min.

V. Conclusion

The results in this paper proved that the proposed BDCE control method for multi-phase induction machine drives works remarkably well in the sub-base and flux weakening speed regions of the drive. A linear relationship between the torque and torque current is found both in the analysis and through measurements. The current controller is effective even in the flux weakening speed region. The torque sensitivity to changes in the control gain are minimal which is good since the control gain depends on the rotor bar resistance, which may vary by up to 40 % due to temperature changes.

In particular, it is found that the number of field phases can rather be reduced for better use of the inverter current capability and for better current density distribution. The overall efficiency of the proposed multiphase induction machine drive is found to be lower, but within 3 % of that of the conventional three-phase drive system.

The BDCE control method is suitable for very large drives, utilising high phase numbers. The main reason for this is its simplicity when compared to the increasing complexity of available control methods with increase in the number of phases, e.g. up to15 phases. As described in the paper, it has been proved that the BDCE control method can be used for cage and wound rotor multiphase induction machines.

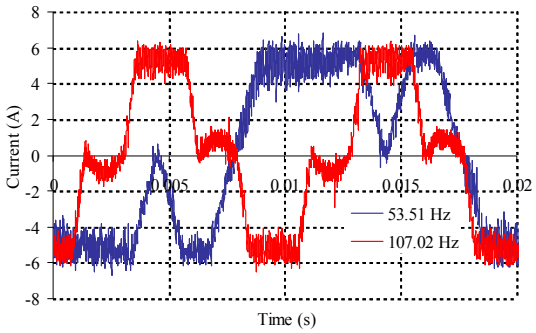

Fig. 8. Measured stator phase current waveforms of the 9-phase induction machine at a dc bus voltage of V_{dc} = 400 V. Blue: at rated flux, rated load [I_f = 5.83 A, I_t = 5.5 A, k = 0.638, T = 67 Nm] and rated speed (1500 r/min); Red: in flux weakening at double rated speed (3000 r/min) and half rated load [I_f = 1.1 A, I_t = 5.5 A, k = 1.28].

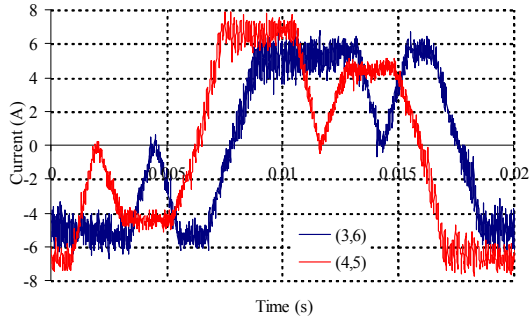

Fig. 9. Measured stator phase current waveforms of the 9-phase induction machine at a dc bus voltage of Vdc = 400 V. Blue: Flux phases m_f = 3, torque phases m_t = 6, m = 3/6 = 0.5 [I_f = 5.83 A, I_t = 5.5 A, rated flux density, rated torque]; Red: Flux phases m_f = 4, torque phases m_t = 5, m = 4/5 = 0.8 [I_f = 4.68 A, I_t = 6.83 A, rated flux density, rated torque];

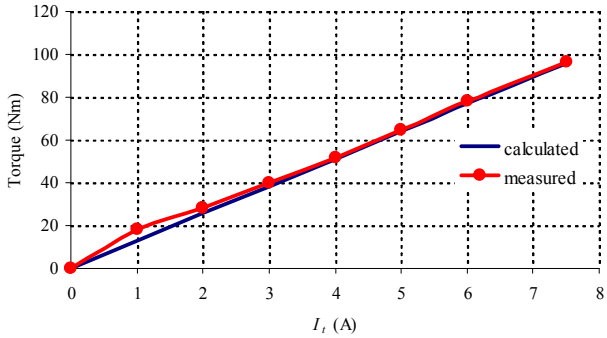

Fig. 10. Comparison of the measured and calculated torque versus torque current (I_t), with I_f = 5.83 A, k = 0.638 and speed = 500 r/min.

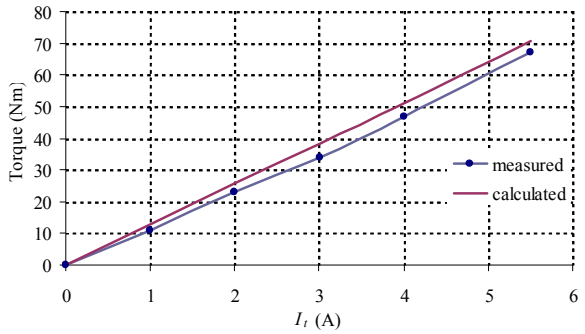

Fig. 11. Comparison of measured and calculated torque versus torque current, with I_f = 5.83 A, k = 0.638 and speed = 1500 r/min.

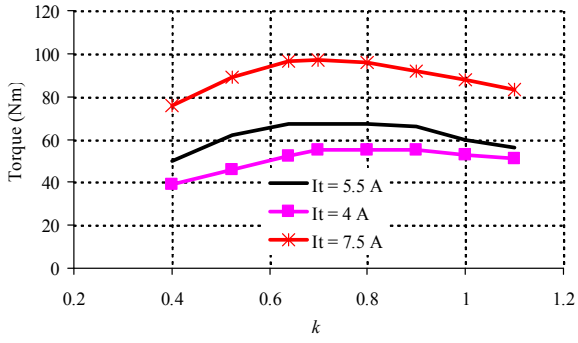

Fig. 12. Measured effect (at 500 r/min) of the k-value (control gain) on torque with I_t a parameter. Rated k-value is k = 0.638 and rated I_t-value is I_t= 5.5 A.

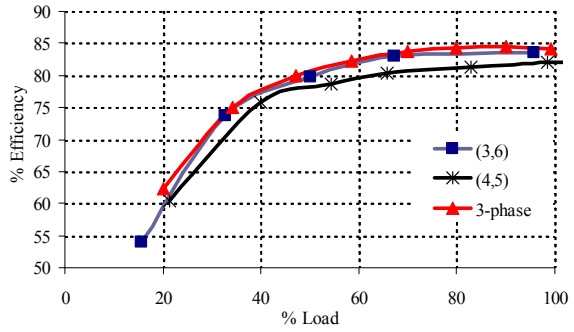

Fig. 13. Measured efficiency of the system (converter and induction machine) versus percentage torque load for (i) m = 0.5 (m_f = 3, m_t = 6) , (ii) m = 0.8 (m_f = 4, m_t = 5) and (iii) a standard 11 KW 3-phase induction machine drive under V/Hz control.

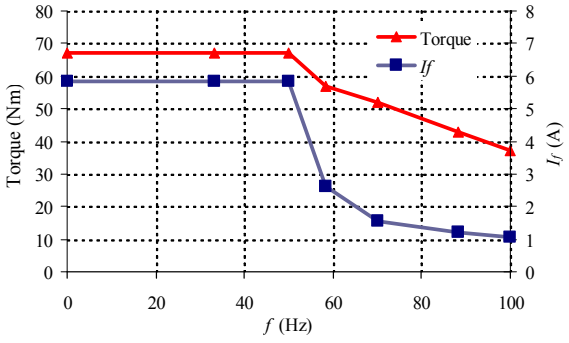

Fig. 14. Measured torque and field current versus frequency with I_t = 5.5 A.

REFERENCES

[1] E. Levi, "Recent developments in high performance speed multiphase induction motor drives," in Sixth International Symposium Nikola Tesla. 2006.

[2] G. K. Singh, "Multi-phase induction machine drive research - a survey." Elsevier Electric Power Systems Research, 2002: p. 139-147.

[3] H. A. Toliyat and T. A. Lipo, "Analysis of concentrated winding induction machines for adjustable speed drive applications-experimental results." IEEE Transactions on Energy Conversion, 1994. vol. 9, no. 4: p. 695-700.

[4] E. Levi, R. Bojoi, F. Profumo, H. A. Toliyat, and S. Williamson, "Multiphase induction motor drives - a technology status review." IEE Proceedings - Electric Power Applications, 2007. vol. 1, no. 4: p. 489-516.

[5] A. C. Smith, S. Williamson, and C. G. Hodge. "High torque dense naval propulsion motors." Proc. IEEE International Electric Machines and Drives Conference IEMDC,. 2003.

[6] M. Jones, S. N. Vukosavic, and E. Levi, "Parallel-connected multiphase multidrive systems with single inverter supply." IEEE Transactions on Industrial Electronics, 2009. vol. 56, no. 6: p. 2047 - 2057.

[7] H. Xu, H. A. Toliyat, and L. J. Petersen. "Rotor field oriented control of five-phase induction motor with the combined fundamental and third harmonic currents." 16th Annual IEEE Applied Power Electronics Conference and Exposition, APEC 2001. 2001.

[8] R. O. C. Lyra and T. A. Lipo, "Torque density improvement in a six-phase induction motor with third harmonic current injection." IEEE Transactions on Industry Applications, 2002. vol. 38, no. 5: p. 1351-1360.

[9] G. W. McLean, G. F. Nix, and S. R. Alwash, "Performance and design of induction motors with square-wave excitation." IEE Proceedings, 1969. vol. 116, no. 8: p. 1405 - 1411.

[10] H. A. Toliyat, T. A. Lipo, and J. C. White, "Analysis of a concentrated winding induction machine for adjustable speed drive applications: Part 1 (motor analysis)." IEEE Transactions on Energy Conversion, 1991. vol. 6: p. 679-683.

[11] F. Terrien, S. Siala, and P. Noy. "Multiphase induction motor sensorless control for electric ship propulsion." Proc. IEE Power Electronics, Machines and Drives Conference. PEMD. 2004. Edinburgh, Scotland.

[12] R. I. Jones. "The more electric aircraft: The past and the future?" IEE Colloquium on Electrical Machines and Systems for the More Electric Aircraft. 1999.

[13] M. J. J. Cronin, "The all-electric aircraft." IEE Review, 1990. vol. 36: p. 3.9-311.

[14] L. de Lillo, L. Empringham, P. W. Wheeler, S. Khwan-On, C. Gerada, M. N. Othman, and X. Huang, "Multiphase power converter drive for fault-tolerant machine development in aerospace applications." IEEE Transactions on Industrial Electronics, 2010. vol. 57, no. 2: p. 575 - 583.

[15] U. C. Mupambireyi, N. P. van der Duijn Schouten, B. M. Gordon, and R. A. McMahon. "High phase number induction motor drives for battery applications." The 8th International Conference on Power Electronocs and Variable Speed Drives. 2000. London, UK.

[16] Y. Ai, M. J. Kamper, and A. D. Le Roux, "Novel direct flux and direct torque control of six-phase induction machine with nearly square air gap flux density." IEEE Transactions on Industry Applications, 2007. vol. 43, no. 6: p. 1534-1543.

[17] L. Weichao, H. An, G. Shiguang, and S. Chi. "Rapid control prototyping of fifteen-phase induction motor drives based on dspace." International Conference on Electrical Machines and Systems, ICEMS 2008. 2008.

[18] N. Gule and M. J. Kamper. "Optimal ratio of field to torque phases in multi-phase induction machines using special phase current waveforms." Proceedings of International Conference on Electrical Machines (ICEM2008). 2008.